ACS Infectious Diseases

pubs.acs.org/journal/aidcbc

Article

A Supramolecular Platform Technology for Bacterial Cell Surface Modification

Nikolas Duszenko, Danny M. van Willigen, Mick M. Welling, Clarize M. de Korne, Roos van Schuijlenburg, Beatrice M.F. Winkel, Fijs W.B. van Leeuwen, and Meta Roestenberg*

Cite This: *ACS Infect. Dis.* 2020, 6, 1734–1744

Read Online

ACCESS | Metrics & More | Article Recommendations | Supporting Information

ABSTRACT: In an era of antimicrobial resistance, a better understanding of the interaction between bacteria and the sentinel immune system is needed to discover new therapeutic targets for combating bacterial infectious disease. Sentinel immune cells such as macrophages phagocytose intact bacteria and thereby initiate ensuing immune responses. The bacterial surface composition is a key element that determines the macrophage signaling. To study the role of the bacterial cell surface composition in immune recognition, we developed a platform technology for altering bacterial surfaces in a controlled manner with versatile chemical scaffolds. We show that these scaffolds are efficiently loaded onto both Gram-positive and -negative bacteria and that their presence does not impair the capacity of monocyte-derived macrophages to phagocytose bacteria and subsequently signal to other components of the immune system. We believe this technology thus presents a useful tool to study the role of bacterial cell surface composition in disease etiology and potentially in novel interventions utilizing intact bacteria for vaccination.

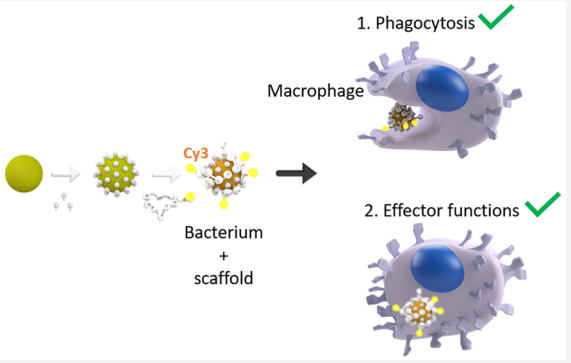

KEYWORDS: *bacteria, infectious disease, surface modification, supramolecular chemistry, immune response*

The rise of drug-resistant bacteria has led to the reemergence of bacterial infectious diseases once thought vanquished with the discovery of antibiotics.[1] Novel vaccines and drugs are needed to combat this growing threat. A better understanding of the interactions between bacteria and the immune system can facilitate the identification of new targets for interventions.

Interactions between bacteria and the immune system are initiated by cells of the innate immune system, such as macrophages (MΦs). These cells are responsible for orchestrating the ensuing immune response.[2] MΦs are able to recognize bacteria by their size and unique bacterial cell wall components.[3,4] These features prompt the MΦ to internalize the bacteria by phagocytosis and degrade them. Doing so liberates the bacterial cell wall components, which dose-dependently trigger intracellular signaling cascades that modulate MΦ effector functions.[5] The bacterial cell wall composition is thus thought to be responsible for the large heterogeneity in bacteria–host interactions, ranging from the vigorous systemic inflammatory response syndromes seen with Gram-negative bacteria such *Escherichia coli* to the comparatively weak responses to many Gram-positive bacteria like *Staphylococcus aureus*.[6,7]

A single bacterial cell surface component of Gram-negative bacteria, lipopolysaccharide (LPS), is responsible for the previously mentioned systemic inflammatory response syndromes. LPS potency in priming immune responses has been utilized in vaccine development, where chemically modified LPS variants have been successfully used to create potent new vaccines for hepatitis B and human papillomavirus.[8,9] Bacteria like the Gram-positive *S. aureus* lack highly immunogenic components such as LPS, resulting in dampened immune responses that allow *S. aureus* to establish chronic infections that the immune system is unable to clear.[10,11] Other pathogenic bacteria have instead evolved modifications of immunogenic components that render them inert. There are, for example, a number of Gram-negative bacterial species, like *Salmonella enterica* and *Helicobacter pylori*, whose unusual LPS structure does not elicit a proper immune response.[12] Much like *S. aureus*, these bacteria can establish chronic infections. Further unraveling which bacterial cell wall components are responsible for directing MΦ responses is thus an important step in advancing our understanding of interactions between bacteria and the immune system.

Received: December 29, 2019
Published: May 4, 2020

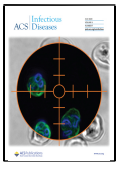

https://dx.doi.org/10.1021/acsinfecdis.9b00523
ACS Infect. Dis. 2020, 6, 1734–1744

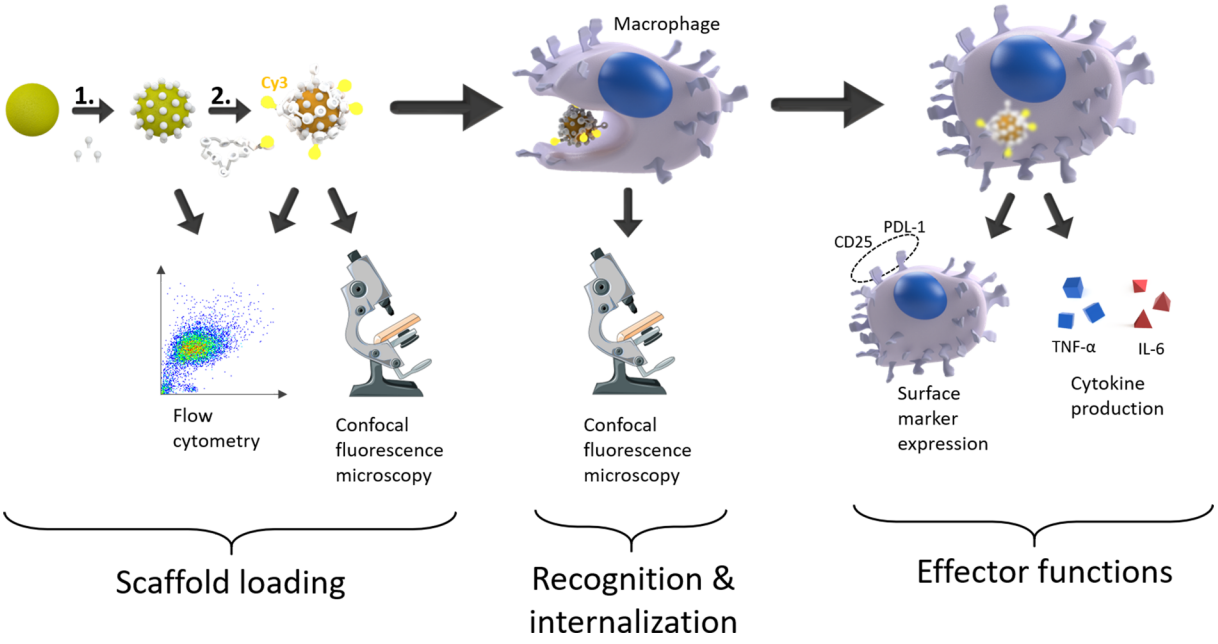

Figure 1. Experimental setup of the described study. Schematic illustrating the process by which the scaffold $\mathbf{Cy3_{1.5}CD_{100}PIBMA_{389}}$ was loaded onto three different entities, and its concomitant effects on immune responses were assessed. The surface of each entity was first functionalized with (1) adamantane, followed by (2) $\mathbf{Cy3_{1.5}CD_{100}PIBMA_{389}}$ loading. The presence of the loaded scaffold was then confirmed by flow cytometry and confocal fluorescence microscopy. Thereafter, the ability of MoMΦ to recognize and internalize $\mathbf{Cy3_{1.5}CD_{100}PIBMA_{389}}$-loaded entities was analyzed by confocal fluorescence microscopy. Finally, MoMΦ effector functions in response to $\mathbf{Cy3_{1.5}CD_{100}PIBMA_{389}}$-loaded entities, as gauged by surface marker expression and cytokine production, were assessed. Blue boxes represent the cytokine TNF-α, and red triangles represent the cytokine IL-6. Microscope adapted with permission under a Creative Commons Attribution 3.0 Unported License from Servier Medical Art.

To study the role of bacterial cell wall components in early immune responses, we envisioned a tool that would allow us to alter the bacterial cell wall in a controlled manner without disturbing the bacteria's structural integrity. The reproducible chemical modification of (bacterial) cell surfaces is in itself a challenging endeavor, but doing so in the context of introducing immunomodulatory compounds presents unique challenges.[13−15] As immune responses are influenced by immunomodulator quantity, it is essential to clearly define loading rates. One way of doing this is by using a generic chemical platform that standardizes the loading rate regardless of the compound being introduced. Recently, we have developed pretargeting methods that enable precise quantification of the loading rate. By harnessing supramolecular chemistry, we reproducibly loaded macro-aggregated albumin (MAA) microparticles and eukaryotic cells with scaffolds that remained stable under chemically challenging *in vitro* and *in vivo* conditions.[16−18] The multivalent host−guest interactions between β-cyclodextrin (CD) and adamantane (Ad) underpinning these scaffolds have already found widespread use for controllably introducing various chemical and biological functionalities onto the inorganic surface.[19−21] We thus reasoned that these scaffolds might similarly be used as a generic chemical platform for controllably introducing (immunomodulatory) components onto bacterial cells while preserving the viability and original biological composition.

The aim of this study was to investigate the use of supramolecular scaffolds as a generic chemical platform to modify the bacterial cell surface composition. To this end, we first assessed the loading of our supramolecular scaffolds onto both Gram-positive (*Staphylococcus aureus*) and Gram-negative (*Escherichia coli*) bacteria, using MAA microspheres as a validated control. We then assayed the effects of these scaffolds on MΦ responses.

RESULTS

In this study we used three different entities to investigate the loading of a chemical scaffold $\mathbf{Cy3_{1.5}CD_{100}PIBMA_{389}}$ onto bacterial cell surfaces and the resultant effects on MΦ recognition and response, as gauged by three major immunological parameters, phagocytosis, surface marker expression, and cytokine production, using a monocyte-derived MΦ (MoMΦ) assay (Figure 1).

$\mathbf{Cy3_{1.5}CD_{100}PIBMA_{389}}$ is a Versatile Scaffold That Is Efficiently Loaded onto Both Gram-Positive and -Negative Bacteria. Our experimental setup was first validated using 10−20 μm MAA microspheres. To assess whether functionalizing MAA by conjugating Ad to the primary amines of lysine residues via amide linkages was a promising strategy, we used an analogous reagent to couple Cy5 to MAA via amide linkages. A flow cytometric analysis of the resulting Cy5 signal showed this to be an efficient process (Figure 2ai and 2aii). We next confirmed the loading of $\mathbf{Cy3_{1.5}CD_{100}PIBMA_{389}}$ onto Ad-functionalized MAA by confocal fluorescence microscopy (Figure 3a). A flow cytometric analysis showed the $\mathbf{Cy3_{1.5}CD_{100}PIBMA_{389}}$ loading (Figure 4ai) to be highly efficient, resulting in 98.5 ± 0.25% MAA particles loaded with $\mathbf{Cy3_{1.5}CD_{100}PIBMA_{389}}$, and demonstrated that Ad functionalization facilitated $\mathbf{Cy3_{1.5}CD_{100}PIBMA_{389}}$ loading by more than 2-fold (3,556 ± 224 vs 1,606 ± 668, $p < 0.01$, Figure 4aii).

We subsequently moved onto transferring our technology to *Staphylococcus aureus*, a Gram-positive bacterium, and *Escherichia coli*, a Gram-negative bacterium. Doing so involved an alternative Ad functionalization, where Ad was first conjugated

https://dx.doi.org/10.1021/acsinfecdis.9b00523
ACS Infect. Dis. 2020, 6, 1734−1744

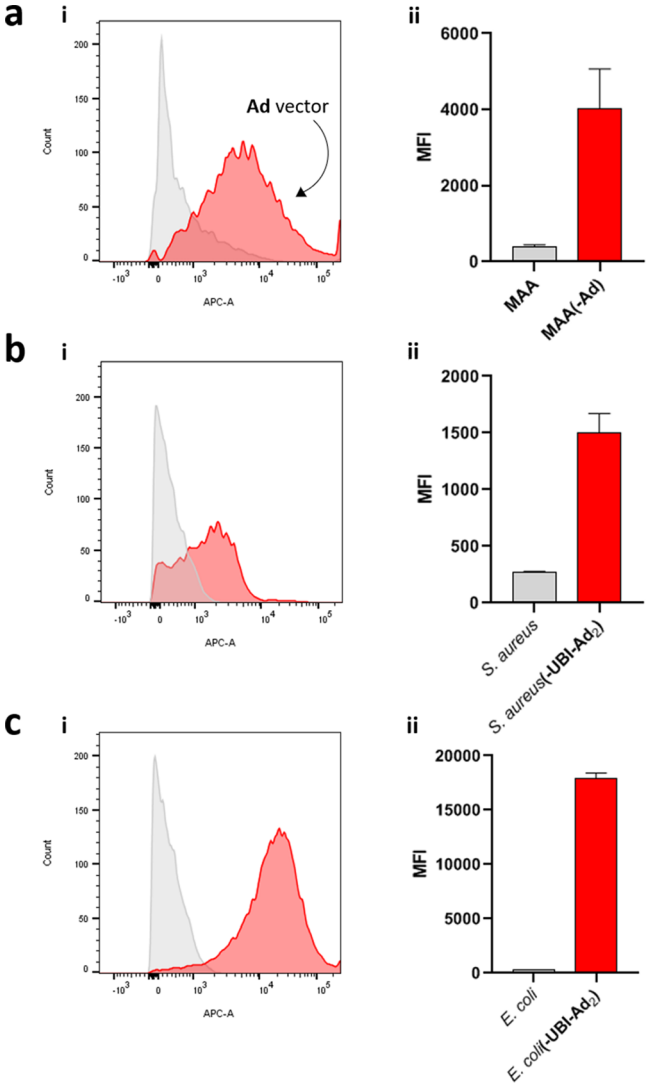

Figure 2. Ad functionalization efficiency for (a) MAA, (b) *S. aureus*, and (c) *E. coli*. Potential Ad functionalization efficiency was assessed with the use of Cy5-labeled vectors (amide bond for MAA, UBI_{29-41} for bacteria) onto MAA/bacterial surfaces. After functionalization, Cy5 signals were measured on a flow cytometer (i). Median fluorescent intensities (MFI) of these Cy5 signals for functionalized MAA or bacteria (red) versus unlabeled controls (gray) are given in (ii) as the mean ± standard deviation for a representative experiment of $n = 3$. Ad = adamantane, MAA = macro-aggregated albumin.

to a cationic peptide (UBI_{29-41}) known to insert itself into bacterial cell membranes that served as a vector for then introducing Ad onto the bacterial cell surface.[22] We assessed the feasibility of this approach using a Cy5-labeled UBI_{29-41}, and via flow cytometry, we observed UBI_{29-41} to be efficiently incorporated into both *S. aureus* (Figure 2bi and 2bii) and *E. coli* (Figure 2ci and 2cii). Following this validation, we confirmed the loading of $\mathbf{Cy3_{1.5}CD_{100}PIBMA_{389}}$ via confocal fluorescence microscopy onto both Ad-functionalized *S. aureus* (Figure 3b) and *E. coli* (Figure 3c), as evinced by clear Cy3 surface signals that contrasted with the Hoechst counterstaining of the cells' cytoplasm (Figure 3d and 3e); this pattern was consistently observed among bacteria (Figure S1). A subsequent flow cytometry analysis showed $\mathbf{Cy3_{1.5}CD_{100}PIBMA_{389}}$ loading rates of 99.5 ± 0.1% for *S. aureus* (Figure 4bi) and 96.4 ± 1.4% for *E. coli* (Figure 4ci). There was a discrepancy between our bacterial platforms regarding the importance of Ad functionalization for facilitating $\mathbf{Cy3_{1.5}CD_{100}PIBMA_{389}}$ loading: Ad_2-UBI_{29-41} surface functionalization enhanced $\mathbf{Cy3_{1.5}CD_{100}PIBMA_{389}}$ loading to Gram-positive *S. aureus* more than 3-fold (51786 ± 1999 vs 17464 ± 1273, $p < 0.01$, Figure 4bii), whereas the increase was less than 2-fold for Gram-negative *E. coli* (64519 ± 10083 vs 46456 ± 7290, $p = 0.07$, Figure 4cii).

Previously, supramolecular host−guest chemistry on cell surfaces has been shown to not adversely affect cell viability.[16] We similarly did not note any adverse effects of $\mathbf{Cy3_{1.5}CD_{100}PIBMA_{389}}$ loading on the viability for *S. aureus*, as gauged by colony counts (12.8 ± 2.9 vs 12 ± 3.3, $p = 0.66$, Figure 5a). However, *E. coli* viability did appear hampered by scaffold loading (4.5 ± 1.5 vs 13.2 ± 7.7, $p = 0.022$, Figure 5b).

$\mathbf{Cy3_{1.5}CD_{100}PIBMA_{389}}$ Loading Does Not Interfere with the Core Functionalities of Monocyte-Derived Macrophages. To assess whether $\mathbf{Cy3_{1.5}CD_{100}PIBMA_{389}}$ loading adversely affects the functioning of (sentinel) immune cells, we first examined via confocal microscopy the response of monocyte-derived macrophages (MoMΦ) to our $\mathbf{Cy3_{1.5}CD_{100}PIBMA_{389}}$-loaded MAA/bacteria. $\mathbf{Cy3_{1.5}CD_{100}PIBMA_{389}}$-loaded MAA particles were readily phagocytosed within 10 min, an illustration of which can be seen in Figure 6a. The quantitated phagocytosis of $\mathbf{Cy3_{1.5}CD_{100}PIBMA_{389}}$-loaded MAA versus control particles showed the two phagocytosed in comparable quantities (37.5 ± 13.6% vs 30.1 ± 9.9%, $p = 0.491$). Similarly, we found that $\mathbf{Cy3_{1.5}CD_{100}PIBMA_{389}}$-loaded *S. aureus* (Figure 6b) and *E. coli* (Figure 6c) were phagocytosed within 10 min, quantitation of which again showed comparable uptake between the loaded and control *S. aureus* (11.1 ± 2.4 vs 14.3 ± 2.7 A.U., $p = 0.194$) and *E. coli* (7.1 ± 1.6 vs 9.6 ± 3.2 A.U., $p = 0.284$). Additional images demonstrating the recognition and internalization of $\mathbf{Cy3_{1.5}CD_{100}PIBMA_{389}}$-loaded *S. aureus* and *E. coli* are provided in Figures S2 and S3.

We next assayed the effects of loaded $\mathbf{Cy3_{1.5}CD_{100}PIBMA_{389}}$ on the typical effector functions of MoMΦ: surface marker expression and cytokine production. When stimulated with $\mathbf{Cy3_{1.5}CD_{100}PIBMA_{389}}$-loaded MAA particles, MoMΦ displayed similar dose-dependent responses in the surface marker expression of CD25 and PDL-1, as seen in response to the control MAA particles. At high particle concentrations (1:1 ratio with MoMΦ) both CD25 (2.20 ± 0.55 vs 1.25 ± 0.22 fold-change, Figure 7ai) and PDL-1 (3.02 ± 0.35 vs 1.90 ± 0.19 fold-change, Figure 7aii) expression were elevated in response to $\mathbf{Cy3_{1.5}CD_{100}PIBMA_{389}}$-loaded MAA particles. Cytokine production also showed increases in TNF-α (281.1 ± 197.8 vs 87.8 ± 48.4 pg/mL, Figure 8ai) and IL-6 (1,402 ± 269.3 vs 616.7 ± 135.6 pg/mL, Figure 8aii) in response to $\mathbf{Cy3_{1.5}CD_{100}PIBMA_{389}}$-loaded MAA particles at a 1:1 ratio with MoMΦ. However, both increases in surface marker expression and cytokine production were not comparable to responses in positive controls (LPS- and IFN-γ-stimulated MoMΦ), suggesting that their relevance might be limited. Analogous results were obtained when MoMΦ was stimulated with soluble $\mathbf{Cy3_{1.5}CD_{100}PIBMA_{389}}$ alone (data not shown).

Similar responses were seen in MoMΦ exposed to $\mathbf{Cy3_{1.5}CD_{100}PIBMA_{389}}$-loaded versus control *S. aureus*. Dose-dependent increases in surface marker expression were again elevated in response to $\mathbf{Cy3_{1.5}CD_{100}PIBMA_{389}}$-loaded *S. aureus*, especially at high concentrations (4:1 ratio of bacteria

https://dx.doi.org/10.1021/acsinfecdis.9b00523
ACS Infect. Dis. 2020, 6, 1734−1744

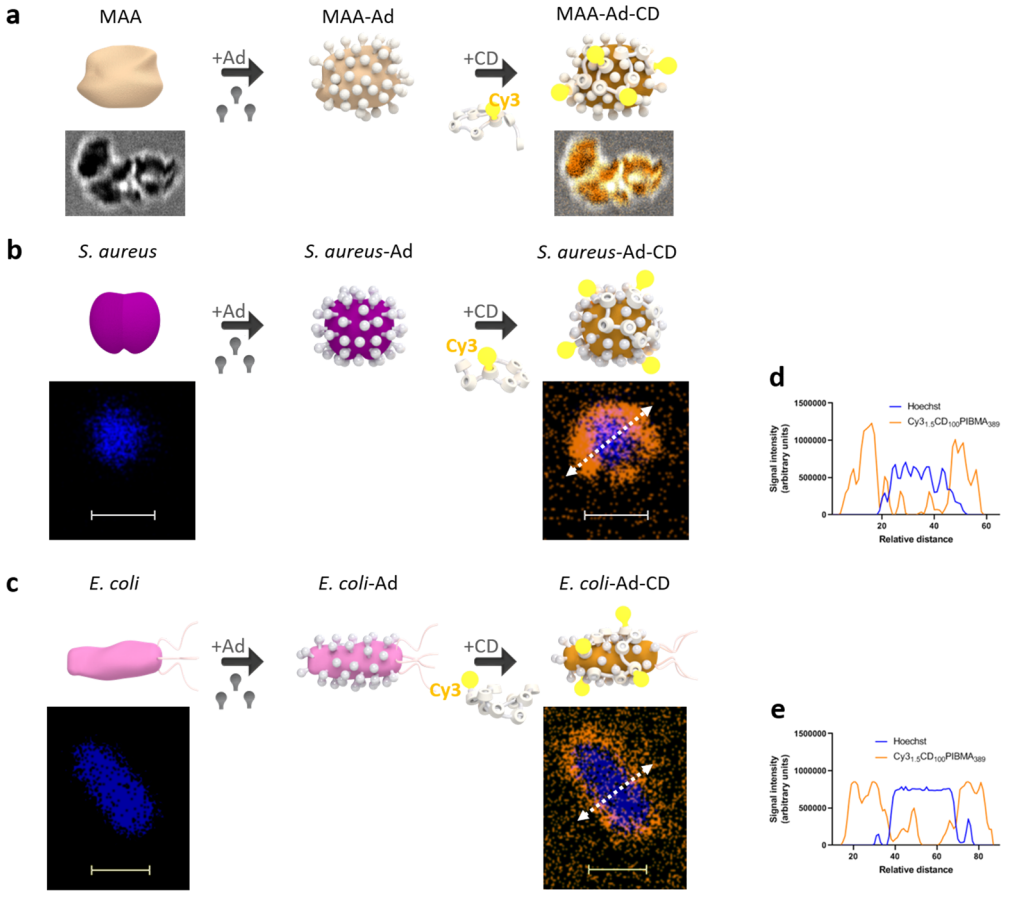

Figure 3. $Cy3_{1.5}CD_{100}PIBMA_{389}$ loading onto (a) a microbial model and (b) (c) two different bacteria. Confocal fluorescence microscopy demonstrating the presence of $Cy3_{1.5}CD_{100}PIBMA_{389}$ loaded onto (a) MAA; (b) *S. aureus*, a typical Gram-positive bacterium; and (c) *E. coli*, a typical Gram-negative bacterium. To assess the location of $Cy3_{1.5}CD_{100}PIBMA_{389}$ on the bacteria, the fluorescent signal intensities of Cy3 and Hoechst in a cross section of the bacteria were analyzed and plotted for (d) *S. aureus* and (e) *E. coli*. Scale bar = 1 μm. Ad = adamantane, CD = $Cy3_{1.5}CD_{100}PIBMA_{389}$, MAA = macro-aggregated albumin.

to MoMΦ), as seen with increases of CD25 (2.27 ± 0.56 vs 1.4 ± 0.29 fold-change, Figure 7bi) and PDL-1 (2.58 ± 0.49 vs 1.46 ± 0.28 fold-change, Figure 7bii) expression. Cytokine production showed a similar dose-dependent pattern, which at a 4:1 ratio of bacteria to MoMΦ resulted in increases in TNF-α (518.67 ± 394.8 vs 216.7 ± 81.1 pg/mL, Figure 8bi) and IL-6 (28.1 ± 23.9 vs 4.1 ± 4.9 ng/mL, Figure 8bii). Notably, cytokine production was also influenced by Ad functionalization itself: TNF-α production in response to Ad-functionalized *S. aureus* was nearly as high at a 4:1 ratio as that seen in response to $Cy3_{1.5}CD_{100}PIBMA_{389}$-loaded *S. aureus* (319.6 ± 197.6 vs 518.67 ± 394.8 pg/mL, Figure 8bi), and IL-6 production was comparable (29.1 ± 19.5 vs 28.1 ± 23.9 ng/mL, Figure 8bii). At lower (1:1 ratio) bacterial concentrations, TNF-α production was actually somewhat higher in response to Ad-functionalized *S. aureus* versus $Cy3_{1.5}CD_{100}PIBMA_{389}$-loaded *S. aureus* (447.2 ± 511.9 vs 276.0 ± 326.3 pg/mL, Figure 8bi). As with MAA, these increases were of minor magnitudes compared to increases seen in LPS- and IFN-γ-stimulated positive controls.

Responses to $Cy3_{1.5}CD_{100}PIBMA_{389}$-loaded *E. coli* mostly paralleled the dose-dependent responses seen with MAA and *S. aureus*. The dose-dependent increases that were elevated over control *E. coli* were observed for both CD25 and PDL-1 expression. These increases were, however, relatively small compared to the already robust responses to the control bacteria (as is typical of *E. coli*), as seen at high bacterial concentrations (4:1 ratio of bacteria to MoMΦ) for both CD25 (8.02 ± 1.51 vs 6.84 ± 0.79 fold-change, Figure 7ci) and PDL-1 (5.97 ± 1.06 vs 4.69 ± 0.81 fold-change, Figure 7cii). Cytokine production with respect to TNF-α was unaffected by loaded $Cy3_{1.5}CD_{100}PIBMA_{389}$ even at the high bacterial concentration of 4:1 (2043 ± 942 vs 2898 ± 919 pg/mL, Figure 8ci). IL-6 production was also comparable between $Cy3_{1.5}CD_{100}PIBMA_{389}$-loaded and control *E. coli* at high bacterial concentrations (4:1); however, at lower bacterial concentrations (1:1 ratio), loaded $Cy3_{1.5}CD_{100}PIBMA_{389}$ and Ad functionalization appeared to depress IL-6 production (7.6 ± 6.1 vs 22.5 ± 16.5 ng/mL, Figure 8cii).

DISCUSSION

The present study shows that supramolecular host−guest chemistry can be effectively harnessed to load both Gram-positive and-negative bacterial surfaces with a versatile chemical scaffold. The scaffold $Cy3_{1.5}CD_{100}PIBMA_{389}$ loaded onto bacteria did not impair immune recognition of these bacteria by MoMΦs, as gauged by phagocytic capacity, surface marker expression, and cytokine production. This technology may thus be an attractive platform for future investigations requiring precise introduction of immunomodulatory components onto bacterial pathogens.

https://dx.doi.org/10.1021/acsinfecdis.9b00523
ACS Infect. Dis. 2020, 6, 1734−1744

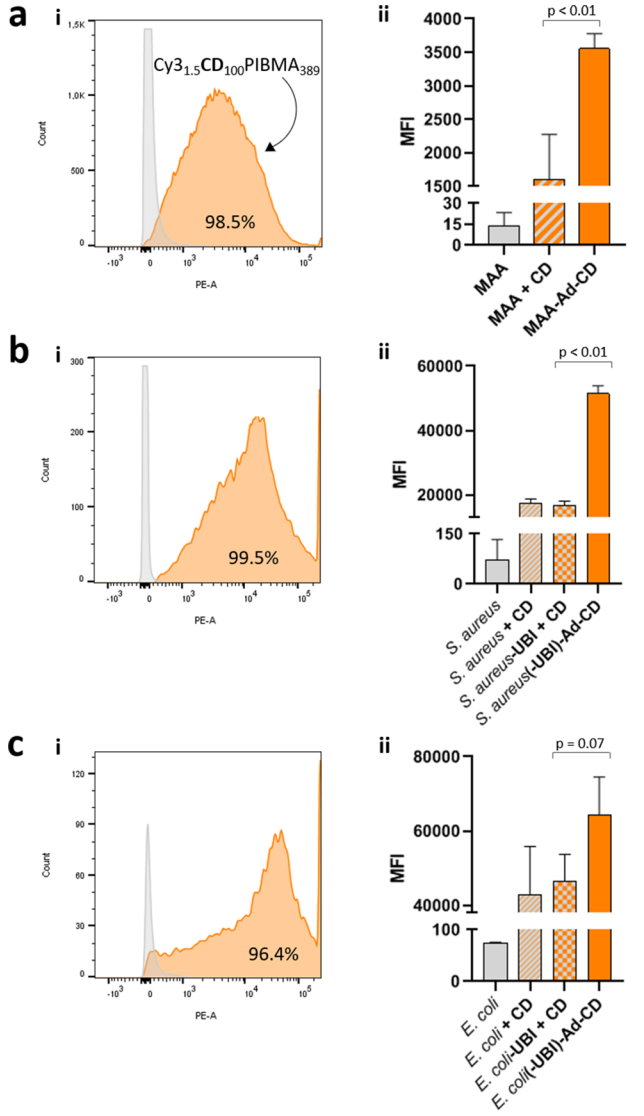

Figure 4. Cy3$_{1.5}$CD$_{100}$PIBMA$_{389}$ loading efficiency for (a) MAA, (b) *S. aureus*, and (c) *E. coli*. Loading was assessed by measuring (i) Cy3 signal intensities on a flow cytometer. Median fluorescent intensities (MFI) of these Cy3 signals for loading in the presence of Ad (orange), loading without Ad but with UBI present (gray/orange checkers), loading without Ad and UBI (gray/orange stripes), and unloaded controls (gray) are given in (ii) as the mean ± standard deviation for a representative experiment of n = 3. CD = Cy3$_{1.5}$CD$_{100}$PIBMA$_{389}$, MAA = macro-aggregated albumin.

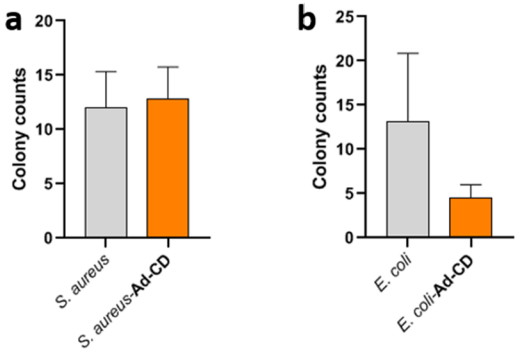

Figure 5. Effect of Cy3$_{1.5}$CD$_{100}$PIBMA$_{389}$ loading on the viability of (a) *S. aureus* and (b) *E. coli*. After Cy3$_{1.5}$CD$_{100}$PIBMA$_{389}$ loading of the bacteria, 10-fold serial dilutions were prepared and plated in 10 μL aliquots onto BHI agar plates. These plates were incubated overnight, and then, colonies at the appropriate dilution were counted. Counts are shown as the mean ± standard deviation of loaded (orange) versus unloaded (gray) bacteria in a representative experiment of n = 6. Ad = adamantane, CD = Cy3$_{1.5}$CD$_{100}$PIBMA$_{389}$.

Existing strategies for modifying bacterial surfaces have generally relied on covalently binding moieties of interest to either cell surface amines/thiols or unnatural chemical ligands, such as aldehydes, introduced metabolically.[13,23,24] Our modification method demonstrates that noncovalent chemistry harnessing supramolecular interactions between CD and Ad is equally able to modify bacterial surfaces and, unlike covalent binding, does not generally perturb the normal functioning of, for example, the cell surface proteins.[13] The introduction of Ad functionalization on the surface of MAA and bacteria significantly promoted the loading of Cy3$_{1.5}$CD$_{100}$PIBMA$_{389}$, particularly for the Gram-positive *S. aureus*, probably because these bacteria lack the highly heterogeneous constituents of Gram-negative surfaces containing certain hydrophobic structures that are able to mimic Ad's supramolecular interactions with CD.[16,25−27]

We found that our cell surface modification method preserved the capacity of MoMΦs to engage and recognize Cy3$_{1.5}$CD$_{100}$PIBMA$_{389}$-loaded MAA and bacteria. Phagocytosis of Cy3$_{1.5}$CD$_{100}$PIBMA$_{389}$-loaded MAA and bacteria was not inhibited by the presence of CD carbohydrates, an important finding for possible future applications of the technology to introduce immunomodulatory components onto bacteria. MoMΦs that phagocytosed Cy3$_{1.5}$CD$_{100}$PIBMA$_{389}$-loaded MAA and bacteria retained their ability to respond normally to these entities, as gauged by surface marker expression and cytokine production. This was most evident in analyzing responses to *E. coli*: robust CD25 and PDL-1 expression and TNF-α production were seen for both control and Cy3$_{1.5}$CD$_{100}$PIBMA$_{389}$-loaded *E. coli*. Altogether, these findings suggest that our Cy3$_{1.5}$CD$_{100}$PIBMA$_{389}$ chemical scaffolds are well-suited for introducing modifications onto bacterial surfaces and can be used to investigate interactions between bacteria and the immune system.

An unexpected finding to emerge from this study was that our Cy3$_{1.5}$CD$_{100}$PIBMA$_{389}$ scaffolds are in themselves somewhat immunogenic. We generally observed dose-dependently increased pro-inflammatory responses to Cy3$_{1.5}$CD$_{100}$PIBMA$_{389}$-loaded MAA, *S. aureus*, and *E. coli*. Remarkably, these increases were most evident with MAA. However, the increases were also notable in bacteria, especially *S. aureus*, with respect to cytokine production. Such disparities between surface markers and cytokines are reflective of the complexity of assessing immune processes using simplified *in vitro* models and indicate the need to ultimately fully evaluate immune responses in more representative *in vivo* models. The immunogenicity of Cy3$_{1.5}$CD$_{100}$PIBMA$_{389}$ is likely mediated by its CD carbohydrates, as studies have identified various immunogenic carbohydrate structures in plants, bacteria, and parasites.[28−30] This is a natural consequence of the important role that carbohydrate diversity plays in the recognition of self- and nonself structures.[31,32] In addition, Ad$_2$-UBI$_{29-41}$ alone also seemed to have a mildly proinflammatory potential, as suggested by the cytokine profiles, possibly mediated by the hydrocarbon components.[33−35] While these unexpected immunogenic properties were interesting to note, they were

https://dx.doi.org/10.1021/acsinfecdis.9b00523
ACS Infect. Dis. 2020, 6, 1734−1744

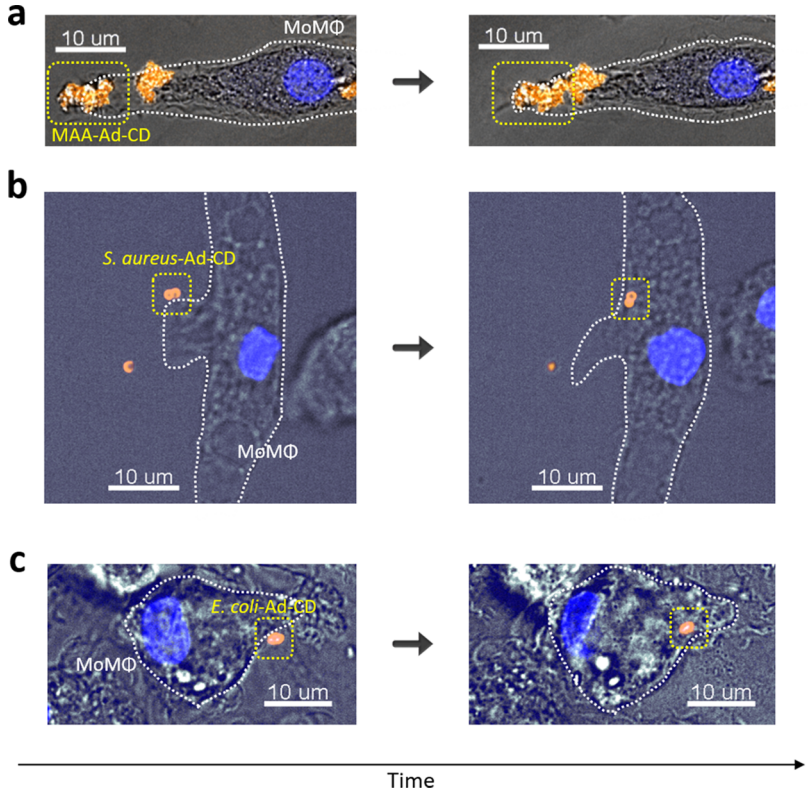

Figure 6. Phagocytic response of MoMΦ to $\mathbf{Cy3_{1.5}CD_{100}PIBMA_{389}}$-loaded (a) MAA, (b) S. aureus, and (c) *E. coli*. Snapshots demonstrating phagocytic uptake by MoMΦ over a course of about 10 min. Ad = adamantane, CD = $\mathbf{Cy3_{1.5}CD_{100}PIBMA_{389}}$, MAA = macro-aggregated albumin, MoMΦ = monocyte-derived macrophage.

very modest compared to positive controls and as such are unlikely to significantly impact the implementation of the presented technology.

Theoretically, the presented technology could be utilized as a tool for adjuvanting (bacterial) whole-organism vaccines. Although whole-organism vaccines generally have less attractive safety profiles, they may be considered for diseases where subunit vaccines provide insufficient protection. The presented technology provides a means of further boosting immune responses to intact bacterial vaccines by physically conjugating immunogenic adjuvants. For instance, introducing LPS-like immunogens onto whole-organism vaccines could, analogously to subunit vaccinology, enhance the immunogenicity of any bacterium.

In conclusion, here, we have shown that supramolecular host−guest chemistry between CD and Ad can be utilized to efficiently load versatile chemical scaffolds onto both Gram-positive and negative bacteria and that these scaffolds are well-tolerated by a canonical immune cell. We thus believe this method provides a useful tool for future investigations seeking to alter the immunogenic properties of (bacterial) pathogens for the purposes of either dissecting the complex host−pathogen interactions involved in infectious disease etiology or developing novel interventions against infectious diseases.

METHODS

Preparation of $\mathbf{Cy3_{1.5}CD_{100}PIBMA_{389}}$-Bound Protein Aggregates and Bacteria. The material characteristics of $\mathbf{Cy3_{1.5}CD_{100}PIBMA_{389}}$, in the context of these experiments, as per recommended guidelines[36] are as follows. $\mathbf{Cy3_{1.5}CD_{100}PIBMA_{389}}$ synthesis was accomplished by grafting the nucleophiles β-CD-NH_2 and Cy3-NH_2 onto the anhydrides of poly(isobutylene-*alt*-maleic-anhydride) in a solution of dry DMSO together with DIPEA, followed by hydrolyzing the nonreacted anhydrides to carboxylates. Thereafter, ethanolamine was conjugated to the free carboxylates via an amide linkage backbone in order to sequester the carboxylates' negative charges, and the product was purified by dialysis. The exact conditions used can be found as previously described.[16] ^{1}H NMR and NMR diffusion ordered spectroscopy (DOSY) determined the product to contain about 100 β-CD units and 1.5 Cy3 units. The product, in linear form, was estimated to be about 240 nm long and 4 nm wide, with a weight of approximately 190 kDa.

To first bind $\mathbf{Cy3_{1.5}CD_{100}PIBMA_{389}}$ to macro-aggregated albumin (MAA), a protein aggregate representing a simplified bacterium, 100 μL of MAA (2 mg/mL) (TechneScan LyoMAA, London, UK), was sonicated (to break up larger aggregates), added to 100 μL of a 1 μM solution of Ad-TFP (tri(2-furyl)phosphine) in PBS supplemented with 2 mg/mL bovine serum albumin (BSA), and incubated for 30 min at 37 °C with shaking. The reaction mixture was centrifuged at 1600 RCF for 3 min; the supernatant was removed, and the pellet was then resuspended in 1 mL of PBS with BSA. Washing was repeated twice. Subsequently, the pellet was resuspended in 100 μL of a 1 μM solution of $\mathbf{Cy3_{1.5}CD_{100}PIBMA_{389}}$ in PBS and incubated for 60 min at 37 °C with shaking. Subsequently, this mixture was similarly washed three times by centrifuging at 1600 RCF for 3 min, removing the supernatant and resuspending the pellet in 1 mL of PBS with BSA. After resuspending the product in 100 μL of PBS with BSA, the concentration in units of particles/mL was determined using a

https://dx.doi.org/10.1021/acsinfecdis.9b00523
ACS Infect. Dis. 2020, 6, 1734−1744

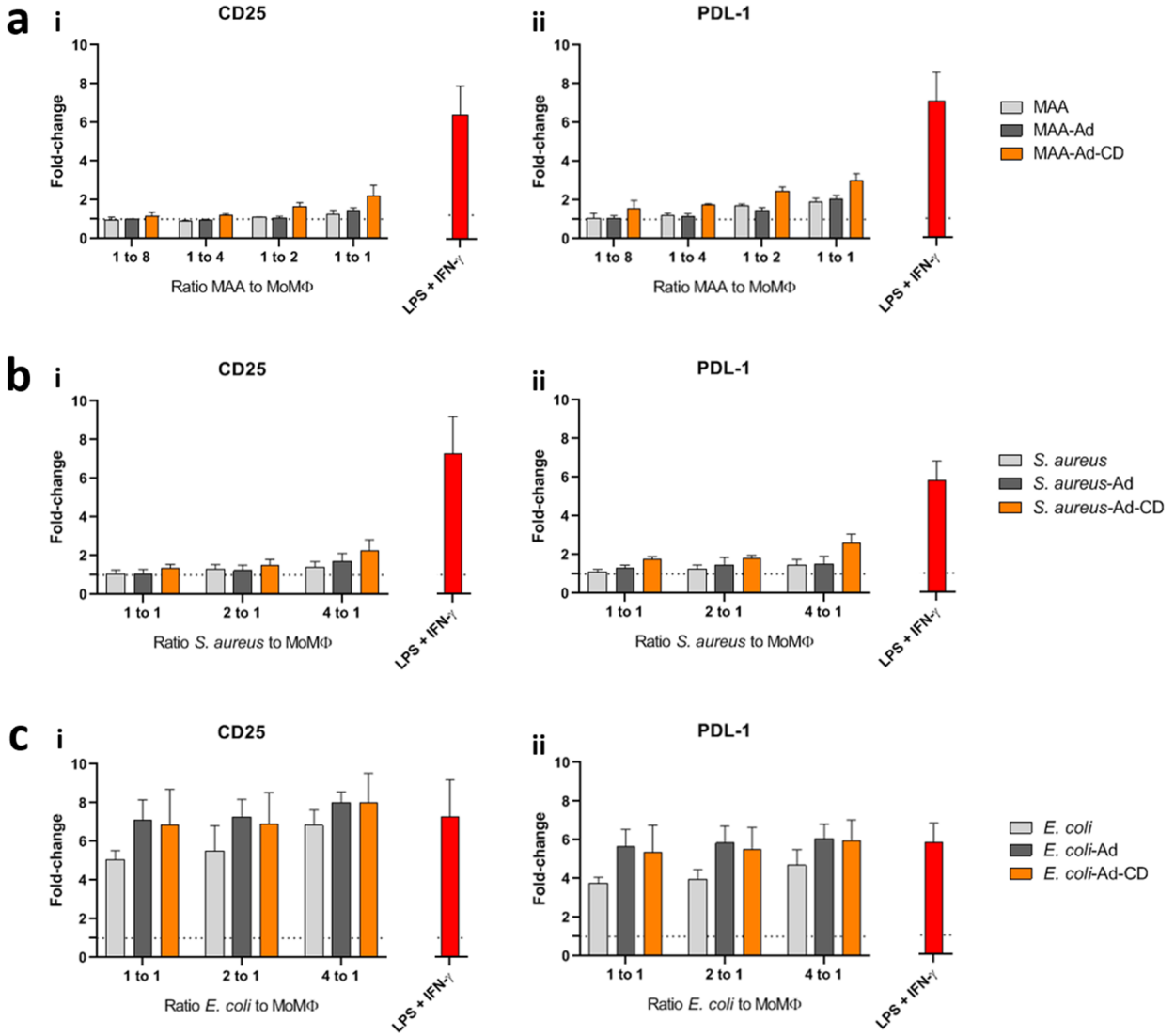

Figure 7. Surface marker responses of MoMΦ to $Cy3_{1.5}CD_{100}PIBMA_{389}$-loaded (a) MAA, (b) *S. aureus*, or (c) *E. coli*. Expression levels of (i) CD25 and (ii) PDL-1 given as fold-change of median fluorescent intensity versus baseline expression in unstimulated MoMΦ by flow cytometry. The control MAA/bacteria are given in light gray, Ad-functionalized controls in dark gray, and loaded MAA/bacteria in orange; positive controls stimulated with LPS and IFN-γ are shown in red. Data are represented as the mean ± standard deviation for representative experiments of $n = 3$. MAA = macro-aggregated albumin, MoMΦ = monocyte-derived macrophages, Ad = adamantane.

Bürker counting chamber. This value was used to prepare eventual dilutions in RPMI (Life Sciences GIBCO, Thermo Fisher Scientific, Waltham, Massachusetts, US) + 10% fetal bovine serum (FBS) (Capricorn Scientific, Ebsdorfergrund, Germany) for analysis by confocal microscopy and flow cytometry.

To initially bind $Cy3_{1.5}CD_{100}PIBMA_{389}$ to bacteria using the Ad functionalization introduced via cell surface lysine residues, 10^7 bacteria (*Staphylococcus aureus* and *Escherichia coli*) were added to 100 μL of a 1 μM solution of Ad-TFP in PBS (also containing 10 μM Hoechst 33342 (Sigma-Aldrich, St. Louis, Missouri, US)), which was then incubated for 30 min at 37 °C with shaking. The reaction mixture was then centrifuged at 10000 RCF for 5 min, and the supernatant was removed; the pellet was resuspended in 1 mL of PBS. Washing was repeated twice. After washing, the pellet was resuspended in 100 μL of a 1 μM solution of $Cy3_{1.5}CD_{100}PIBMA_{389}$ in PBS and incubated for 60 min at 37 °C with shaking. The mixture was then washed thrice with PBS, as described above. After washing, the pellet was resuspended in 100 μL of PBS and analyzed by confocal microscopy.

To alternatively bind $Cy3_{1.5}CD_{100}PIBMA_{389}$ to bacteria using the Ad functionalization introduced via a membrane-adhering ubiquicidin peptide (UBI_{29-41}), 10^7 bacteria were added to 100 μL of a 8 μM solution of UBI-Ad_2 in a 25 mM ammonium acetate buffer of pH 5 (also containing 10 μM Hoechst 33342), which was then incubated for 30 min at 37 °C with shaking. The mixture was then centrifuged at 10000 RCF for 5 min, and the supernatant was removed; the pellet resuspended in PBS. Washing was repeated twice. Subsequently, the pellet was resuspended in 100 μL of a 1 μM solution of $Cy3_{1.5}CD_{100}PIBMA_{389}$ in PBS, which was then incubated for 30 min at 37 °C with shaking. The mixture was then washed 3 times in PBS and finally resuspended in 100 μL of RPMI + 10% FBS to create a stock solution used to prepare dilutions in RPMI + 10% FBS for the analysis by confocal microscopy and flow cytometry.

https://dx.doi.org/10.1021/acsinfecdis.9b00523
ACS Infect. Dis. 2020, 6, 1734−1744

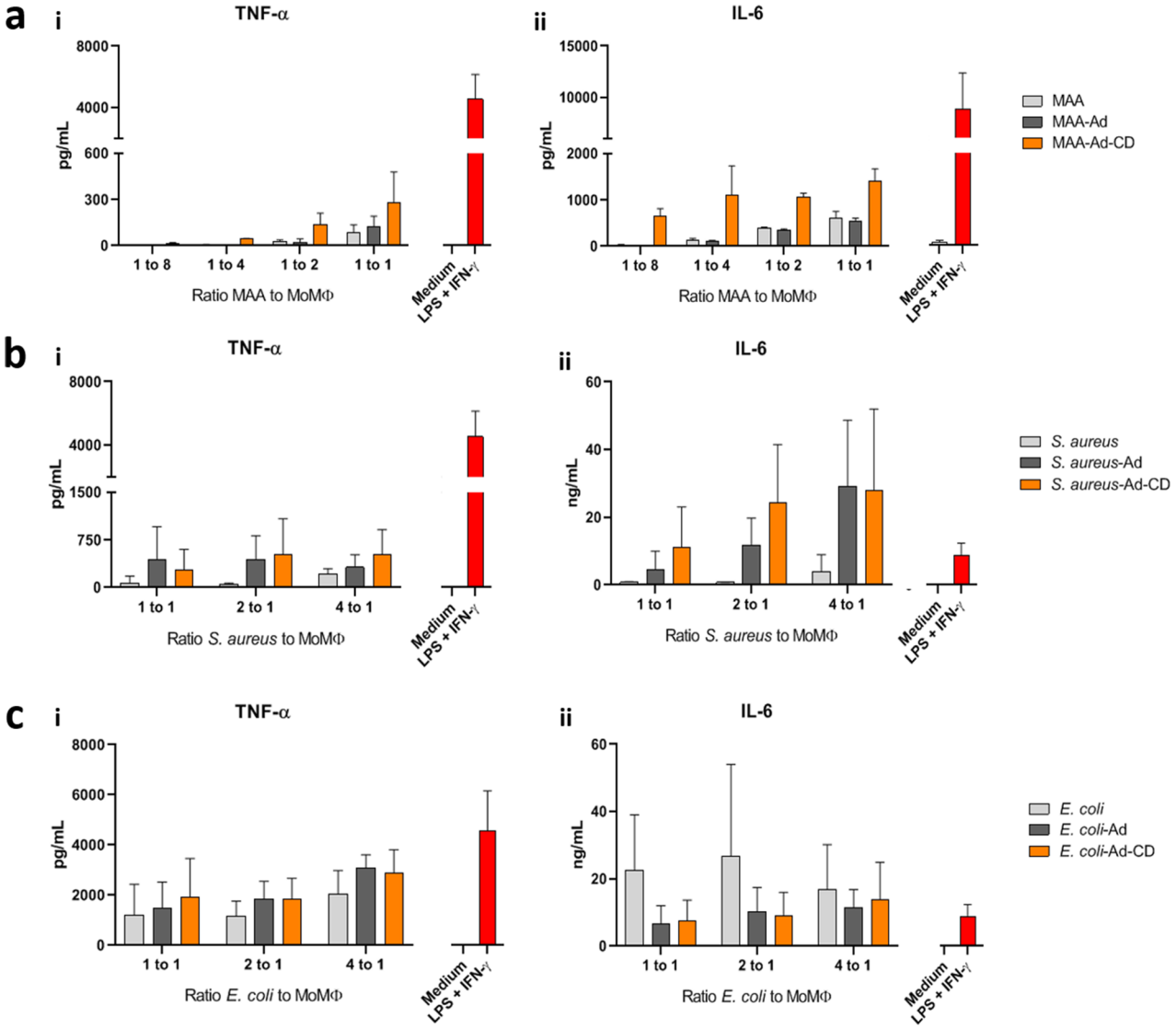

Figure 8. Cytokine responses of MoMΦ to $Cy3_{1.5}CD_{100}PIBMA_{389}$-loaded (a) MAA, (b) *S. aureus*, or (c) *E. coli*. Concentrations of the cytokines (i) TNF-α and (ii) IL-6 in MoMΦ culture supernatants 24 h after stimulation, as measured via ELISA. The control MAA/bacteria are given in light gray, Ad-functionalized controls in dark gray, and loaded MAA/bacteria in orange. MoMΦ stimulated with medium (beige) or LPS and IFN-γ (red) served as negative and positive controls, respectively. Data shown are the mean ± standard deviation for representative experiments of $n = 3$. MAA = macro-aggregated albumin, MoMΦ = monocyte-derived macrophages, Ad = adamantane.

Analysis of $Cy3_{1.5}CD_{100}PIBMA_{389}$-Bound Protein Aggregates and Bacteria. $Cy3_{1.5}CD_{100}PIBMA_{389}$ bound to MAA or bacteria was first qualitatively detected by confocal microscopy performed on a Leica Sp8 WLL confocal microscope using LAS X software. Prior to microscopy, 10 μL inoculums containing ~10^6 units of MAA or bacteria were added to glass-bottom microwell dishes (MatTek Corporation, Ashland, Massachusetts, US), overlaid with 1% agarose pads (to eliminate Brownian motion interfering with digital image acquisition), and finally overlaid with a coverslip.

The quantitation of Ad functionalization and $Cy3_{1.5}CD_{100}PIBMA_{389}$ binding efficiency was performed by flow cytometry on BD (Franklin Lakes, New Jersey, US) LSRFortessa X-20 or FACSCanto II instruments using FACSDiva software using the above-mentioned procedures and reagents or analogues thereof. The bacteria were isolated from debris by gating on their Hoechst signal.

To assess the viability of $Cy3_{1.5}CD_{100}PIBMA_{389}$-bound bacteria, 6.4 × 10^6 CFU/mL bacteria underwent the above-mentioned procedure. These bacteria were then serially diluted 10-fold, and 10 μL inoculums from each dilution were pipetted onto BHI agar plates. These plates were cultured overnight at 37 °C, after which colonies on plates were counted.

Analysis of Phagocytic Responses. MoMΦs were prepared as follows. Peripheral blood from volunteers was diluted 1:1 with room temperature HBSS (Life Sciences GIBCO) containing 100 U/mL penicillin and 100 μg/mL streptomycin. Ficoll (Apotheek AZL, Lokeren, The Netherlands) was added underneath the diluted blood, and samples were spun at 400 RCF for 25 min with slow deceleration. Peripheral blood mononuclear cells (PBMCs) above the Ficoll phase were carefully isolated with a Pasteur pipet and diluted 1:1 with HBSS + 1% fetal bovine serum (FBS). PBMCs were spun at 200 RCF for 20 min. The supernatant was removed, and the pellet was resuspended in HBSS + 1% FBS. PBMCs were again spun at 200 RCF for 20 min. The supernatant was removed, and the pellet was resuspended in MACS buffer (PBS + 0.5% BSA + 2 mM EDTA). After PBMCs were

https://dx.doi.org/10.1021/acsinfecdis.9b00523
ACS Infect. Dis. 2020, 6, 1734−1744

counted, PBMCs were centrifuged at 300 RCF at 4 °C for 10 min. The supernatant was removed, and the cells were resuspended in a 95 μL/10^7 cells MACS buffer. To this suspension, 5 μL/10^7 cells Miltenyi Biotec MACS CD14 microbeads (Cologne, Germany) were added. PBMCs were then incubated for 15 min at 4 °C. After incubation, the cells were washed with a MACS buffer and centrifuged at 300 RCF at 4 °C for 10 min. The supernatant was removed, and the cells were resuspended in 1 mL of MACS buffer; the suspension was run through a Miltenyi Biotec MACS LS column attached to a magnetic separator. The column was washed thrice with MACS buffer. After removing the column from the magnetic separator, the column was flushed with RPMI (Life Sciences GIBCO) containing 100 U/mL penicillin and 100 μg/mL streptomycin. Monocytes were centrifuged at 300 RCF at 4 °C for 10 min. After removing the supernatant, monocytes were resuspended in RPMI + 10% FBS and counted.

To differentiate monocytes into macrophages, monocytes were plated at a density of 400.000 cells/mL in RPMI + 10% FBS supplemented with 20 ng/mL macrophage colony-stimulating factor and incubated at 37 °C. After 2−3 days, the medium was refreshed. After 6 days, macrophages were resuspended by scraping with a pipet tip and counted, after which they were ready for downstream applications.

Confocal microscopy was performed on a Leica Sp8 WLL confocal microscope using LAS X software. One day prior to microscopy, 5 × 10^4 MoMΦs were incubated on glass-bottom microwell dishes (MatTek Corporation) in a 200 μL drop of RPMI + 10% FBS for 2 h at 37 °C. Once the MoMΦs had adhered, an additional 1.8 mL of RPMI + 10% FBS was added, and MoMΦs were incubated at 37 °C overnight. Immediately prior to microscopy the next day, RPMI + 10% FBS was removed from the confocal dish, and a 10 μL inoculum was added to the MoMΦ; a coverslip was overlaid on the cells. MoMΦ behavior was then analyzed in a 37 °C environment.

Analysis of Immune Responses. All experiments were performed in triplicate. MoMΦs postharvesting were plated at a density of 10^5 cells/100 μL in 96-well plates (Thermo Fisher Scientific) and incubated for 24 h at 37 °C. Thereafter, MoMΦs were stimulated with 100 μL of various MAA/*S. aureus*/*E. coli*-Ad-CD dilutions and allowed to incubate for another 24 h at 37 °C. Subsequently, supernatants were removed and stored for an eventual cytokine analysis. Wells were filled with cold PBS, and cells were harvested by scraping with a pipet tip and transferring to a FACS V-bottom plate (Thermo Fisher Scientific). Cells were centrifuged at 350 RCF and 4 °C for 4 min, and the supernatant was discarded. Pellets were resuspended in 50 μL of an Aqua solution (Thermo Fisher Scientific) and incubated on ice for 20 min. Thereafter, 150 μL of 1.9% paraformaldehyde was added, and cells were incubated on ice for 15 min. Cells were centrifuged at 350 RCF and 4 °C for 4 min, and the supernatant was discarded. Pellets were resuspended in 200 μL of PBS and centrifuged at 350 RCF and 4 °C for 4 min, and the supernatant was discarded. Pellets were then resuspended in 30 μL of an antibody mix and incubated for 30 min at 4 °C. After incubation, 170 μL of PBS was added, and cells were centrifuged at 350 RCF and 4 °C for 4 min; the supernatant was discarded. Pellets were resuspended in 50 μL of a FACS buffer (PBS + 0.5% BSA + 2 mM EDTA) and transferred to 1.4 mL FACS tubes. These samples were then run through a BD LSRFortessa X-20 using BD FACSDiva software.

Cytokine production in MoMΦ culture supernatants was assayed using kits from BD Biosciences; specifically, Human TNF ELISA set (Cat. No. 555212) and Human IL-6 ELISA set (Catalogue No. 555220) kits were used according to the manufacturer's specifications and analyzed by a Thermo Fisher Scientific Multiskan FC plate reader.

Statistical Analysis. Mean values were compared by Student's *t* test performed using SPSS 25 software (IBM, Armonk, New York, US).

■ ASSOCIATED CONTENT

Supporting Information

The Supporting Information is available free of charge at https://pubs.acs.org/doi/10.1021/acsinfecdis.9b00523.

Additional images corroborating the findings shown in Figures 3 and 6 of this manuscript (PDF)

■ AUTHOR INFORMATION

Corresponding Author

Meta Roestenberg − *Department of Parasitology and Department of Infectious Diseases, Leiden University Medical Center, Leiden 2333 ZA, The Netherlands*; Email: m.roestenberg@lumc.nl

Authors

Nikolas Duszenko − *Department of Parasitology and Interventional Molecular Imaging Laboratory, Department of Radiology, Leiden University Medical Center, Leiden 2333 ZA, The Netherlands*; orcid.org/0000-0001-7860-1242

Danny M. van Willigen − *Interventional Molecular Imaging Laboratory, Department of Radiology, Leiden University Medical Center, Leiden 2333 ZA, The Netherlands*

Mick M. Welling − *Interventional Molecular Imaging Laboratory, Department of Radiology, Leiden University Medical Center, Leiden 2333 ZA, The Netherlands*; orcid.org/0000-0002-2249-5601

Clarize M. de Korne − *Department of Parasitology and Interventional Molecular Imaging Laboratory, Department of Radiology, Leiden University Medical Center, Leiden 2333 ZA, The Netherlands*

Roos van Schuijlenburg − *Department of Parasitology, Leiden University Medical Center, Leiden 2333 ZA, The Netherlands*

Beatrice M.F. Winkel − *Department of Parasitology, Leiden University Medical Center, Leiden 2333 ZA, The Netherlands*

Fijs W.B. van Leeuwen − *Interventional Molecular Imaging Laboratory, Department of Radiology, Leiden University Medical Center, Leiden 2333 ZA, The Netherlands; Department of Urology, Netherlands Cancer Institute-Antoni van Leeuwenhoek Hospital, Amsterdam 1066 CX, The Netherlands*; orcid.org/0000-0002-6844-4025

Complete contact information is available at: https://pubs.acs.org/10.1021/acsinfecdis.9b00523

Author Contributions

N.D. carried out the experiments and drafted the manuscript. D.M.v.W. synthesized the compounds. M.M.W., C.d.K., R.v.S. and B.M.F.W. helped carry out experiments. F.W.B.v.L. and M.R. helped with the experimental design and critical reading of the manuscript.

Funding

The research leading to these results has received funding from a ZONMW VENI grant (016.156.076) financed by The

Netherlands Organization for Scientific Research (NWO) and an LUMC PhD project grant (18-1919).

Notes

The authors declare no competing financial interest.

■ ACKNOWLEDGMENTS

The authors would like to gratefully acknowledge Sven van Leeuwen for helping them generate the graphics used in this paper.

■ ABBREVIATIONS USED

Ad, adamantane; BHI, brain-heart infusion; CD, β-cyclodextrin; CD25, cluster of differentiation 25; Cy3, cyanine 3; Cy5, cyanine 5; FACS, fluorescence-activated cell sorting; FBS, fetal bovine serum; IL, interleukin; MAA, macro-aggregated albumin; MoMΦ, monocyte-derived macrophage; PAMP, pathogen-associated molecular pattern; PDL-1, programmed death ligand-1; PIBMA, poly(isobutylene-*alt*-maleic-anhydride); RPMI, Roswell Park Memorial Institute (culture medium); TFP, tri(2-furyl)phosphine; UBI, ubiquicidin

■ REFERENCES

(1) Willyard, C. (2017) The drug-resistant bacteria that pose the greatest health threats. *Nature 543*, 15.
(2) Wynn, T. A., Chawla, A., and Pollard, J. W. (2013) Macrophage biology in development, homeostasis and disease. *Nature 496*, 445−455.
(3) Kumar, H., Kawai, T., and Akira, S. (2011) Pathogen recognition by the innate immune system. *Int. Rev. Immunol. 30*, 16−34.
(4) Mogensen, T. H. (2009) Pathogen recognition and inflammatory signaling in innate immune defenses. *Clin Microbiol Rev. 22* (2), 240−273.
(5) Wolf, A. J., and Underhill, D. M. (2018) Peptidoglycan recognition by the innate immune system. *Nat. Rev. Immunol. 18*, 243−254.
(6) Annane, D., Bellissant, E., and Cavaillon, J. M. (2005) Septic shock. *Lancet 365*, 63−78.
(7) Goldmann, O., and Medina, E. (2018) Staphylococcus aureus strategies to evade the host acquired immune response. *Int. J. Med. Microbiol. 308*, 625−630.
(8) Kong, N. C., Beran, J., Kee, S. A., Miguel, J. L., Sanchez, C., Bayas, J. M., Vilella, A., Calbo-Torrecillas, F., Lopez de Novales, E., Srinivasa, K., Stoffel, M., and Hoet, B. (2008) A new adjuvant improves the immune response to hepatitis B vaccine in hemodialysis patients. *Kidney Int. 73*, 856−862.
(9) Paavonen, J, Naud, P, Salmeron, J, Wheeler, C., Chow, S-N, Apter, D, Kitchener, H, Castellsague, X, Teixeira, J., Skinner, S., Hedrick, J, Jaisamrarn, U, Limson, G, Garland, S, Szarewski, A, Romanowski, B, Aoki, F., Schwarz, T., Poppe, W., Bosch, F., Jenkins, D, Hardt, K, Zahaf, T, Descamps, D, Struyf, F, Lehtinen, M, and Dubin, G (2009) Efficacy of human papillomavirus (HPV)-16/18 AS04-adjuvanted vaccine against cervical infection and precancer caused by oncogenic HPV types (PATRICIA): final analysis of a double-blind, randomised study in young women. *Lancet 374* (9686), 301−314.
(10) Bekeredjian-Ding, I., Stein, C., and Uebele, J. (2015) The Innate Immune Response Against Staphylococcus aureus. *Curr. Top. Microbiol. Immunol. 409*, 385−418.
(11) Naber, C. K. (2009) Staphylococcus aureus bacteremia: epidemiology, pathophysiology, and management strategies. *Clin. Infect. Dis. 48*, S231−S237.
(12) Maldonado, R. F., Sa-Correia, I., and Valvano, M. A. (2016) Lipopolysaccharide modification in Gram-negative bacteria during chronic infection. *FEMS Microbiol Rev. 40*, 480−493.
(13) Bi, X., Yin, J., Chen Guanbang, A., and Liu, C. F. (2018) Chemical and Enzymatic Strategies for Bacterial and Mammalian Cell Surface Engineering. *Chem. - Eur. J. 24*, 8042−8050.
(14) Gautam, S., Gniadek, T. J., Kim, T., and Spiegel, D. A. (2013) Exterior design: strategies for redecorating the bacterial surface with small molecules. *Trends Biotechnol. 31*, 258−267.
(15) Mongis, A., Piller, F., and Piller, V. (2017) Coupling of Immunostimulants to Live Cells through Metabolic Glycoengineering and Bioorthogonal Click Chemistry. *Bioconjugate Chem. 28*, 1151−1165.
(16) Rood, M. T., Spa, S. J., Welling, M. M., Ten Hove, J. B., van Willigen, D. M., Buckle, T., Velders, A. H., and van Leeuwen, F. W. (2017) Obtaining control of cell surface functionalizations via Pre-targeting and Supramolecular host guest interactions. *Sci. Rep. 7* (1), 39908.
(17) Spa, S. J., Welling, M. M., van Oosterom, M. N., Rietbergen, D. D. D., Burgmans, M. C., Verboom, W., Huskens, J., Buckle, T., and van Leeuwen, F. W. B. (2018) A Supramolecular Approach for Liver Radioembolization. *Theranostics 8*, 2377−2386.
(18) Welling, M. M., Spa, S. J., van Willigen, D. M., Rietbergen, D. D. D., Roestenberg, M., Buckle, T., and van Leeuwen, F. W. B. (2019) In vivo stability of supramolecular host-guest complexes monitored by dual-isotope multiplexing in a pre-targeting model of experimental liver radioembolization. *J. Controlled Release 293*, 126−134.
(19) Gonzalez-Campo, A., Hsu, S. H., Puig, L., Huskens, J., Reinhoudt, D. N., and Velders, A. H. (2010) Orthogonal covalent and noncovalent functionalization of cyclodextrin-alkyne patterned surfaces. *J. Am. Chem. Soc. 132*, 11434−11436.
(20) Neirynck, P., Brinkmann, J., An, Q., van der Schaft, D. W., Milroy, L. G., Jonkheijm, P., and Brunsveld, L. (2013) Supramolecular control of cell adhesion via ferrocene-cucurbit[7]uril host-guest binding on gold surfaces. *Chem. Commun. (Cambridge, U. K.) 49*, 3679−3681.
(21) Rodell, C. B., Mealy, J. E., and Burdick, J. A. (2015) Supramolecular Guest-Host Interactions for the Preparation of Biomedical Materials. *Bioconjugate Chem. 26*, 2279−2289.
(22) Welling, M. M., Visentin, R., Feitsma, H. I., Lupetti, A., Pauwels, E. K., and Nibbering, P. H. (2004) Infection detection in mice using 99mTc-labeled HYNIC and N2S2 chelate conjugated to the antimicrobial peptide UBI 29−41. *Nucl. Med. Biol. 31*, 503−509.
(23) Dumont, A., Malleron, A., Awwad, M., Dukan, S., and Vauzeilles, B. (2012) Click-mediated labeling of bacterial membranes through metabolic modification of the lipopolysaccharide inner core. *Angew. Chem., Int. Ed. 51*, 3143−3146.
(24) Taherkhani, S., Mohammadi, M., Daoud, J., Martel, S., and Tabrizian, M. (2014) Covalent binding of nanoliposomes to the surface of magnetotactic bacteria for the synthesis of self-propelled therapeutic agents. *ACS Nano 8*, 5049−5060.
(25) Thanassi, D. G., Bliska, J. B., and Christie, P. J. (2012) Surface organelles assembled by secretion systems of Gram-negative bacteria: diversity in structure and function. *FEMS Microbiol Rev. 36* (6), 1046−82.
(26) Whitfield, C., and Trent, M. S. (2014) Biosynthesis and export of bacterial lipopolysaccharides. *Annu. Rev. Biochem. 83*, 99−128.
(27) Hooda, Y., and Moraes, T. F. (2018) Translocation of lipoproteins to the surface of gram negative bacteria. *Curr. Opin. Struct. Biol. 51*, 73−79.
(28) Matsuo, K., Kagaya, U., Itchoda, N., Tabayashi, N., and Matsumura, T. (2014) Deletion of plant-specific sugar residues in plant N-glycans by repression of GDP-D-mannose 4,6-dehydratase and beta-1,2-xylosyltransferase genes. *J. Biosci Bioeng 118*, 448−454.
(29) Pazur, J. H., and Forsberg, L. S. (1980) The sugar sequence of a streptococcal, immunogenic tetraheteroglycan: a revision. *Carbohydr. Res. 83*, 406−408.
(30) Weiss, J. B., Magnani, J. L., and Strand, M. (1986) Identification of Schistosoma mansoni glycolipids that share immunogenic carbohydrate epitopes with glycoproteins. *J. Immunol 136* (11), 4275−4282.

https://dx.doi.org/10.1021/acsinfecdis.9b00523
ACS Infect. Dis. 2020, 6, 1734−1744

(31) Moremen, K. W., Tiemeyer, M., and Nairn, A. V. (2012) Vertebrate protein glycosylation: diversity, synthesis and function. *Nat. Rev. Mol. Cell Biol. 13*, 448−462.
(32) Amon, R., Reuven, E. M., Leviatan Ben-Arye, S., and Padler-Karavani, V. (2014) Glycans in immune recognition and response. *Carbohydr. Res. 389*, 115−122.
(33) Osgood, R. S., Upham, B. L., Bushel, P. R., Velmurugan, K., Xiong, K. N., and Bauer, A. K. (2017) Secondhand Smoke-Prevalent Polycyclic Aromatic Hydrocarbon Binary Mixture-Induced Specific Mitogenic and Pro-inflammatory Cell Signaling Events in Lung Epithelial Cells. *Toxicol. Sci. 157*, 156−171.
(34) Brinchmann, B. C., Skuland, T., Rambol, M. H., Szoke, K., Brinchmann, J. E., Gutleb, A. C., Moschini, E., Kubatova, A., Kukowski, K., Le Ferrec, E., Lagadic-Gossmann, D., Schwarze, P. E., Lag, M., Refsnes, M., Ovrevik, J., and Holme, J. A. (2018) Lipophilic components of diesel exhaust particles induce pro-inflammatory responses in human endothelial cells through AhR dependent pathway(s). *Part. Fibre Toxicol. 15* (1), 21.
(35) Michael, S., Montag, M., and Dott, W. (2013) Pro-inflammatory effects and oxidative stress in lung macrophages and epithelial cells induced by ambient particulate matter. *Environ. Pollut. 183*, 19−29.
(36) Faria, M., Bjornmalm, M., Thurecht, K. J., Kent, S. J., Parton, R. G., Kavallaris, M., Johnston, A. P. R., Gooding, J. J., Corrie, S. R., Boyd, B. J., Thordarson, P., Whittaker, A. K., Stevens, M. M., Prestidge, C. A., Porter, C. J. H., Parak, W. J., Davis, T. P., Crampin, E. J., and Caruso, F. (2018) Minimum information reporting in bio-nano experimental literature. *Nat. Nanotechnol. 13*, 777−785.

https://dx.doi.org/10.1021/acsinfecdis.9b00523
ACS Infect. Dis. 2020, 6, 1734−1744